2004

Mechanical performance of PPy helix tube microactuator

Mehrdad Bahrami Samani
University of Wollongong, mbs87@uow.edu.au

Geoffrey M. Spinks
University of Wollongong, gspinks@uow.edu.au

Christopher David Cook
University of Wollongong, chris_cook@uow.edu.au

Publication Details

Bahrami Samani, M., Spinks, G. Maxwell. & Cook, C. David. (2004). Mechanical performance of PPy helix tube microactuator. In A. Wilson (Eds.), SPIE 5648, Smart Materials III (pp. 163-170). USA: SPIE.

Mechanical performance of PPy Helix Tube micro actuator

Mehrdad Bahrami Samani [a,b], Geoffrey Spinks [a,b] and Christopher Cook* [a]
[a] Faculty of Engineering, University of Wollongong, NSW 2522 AUSTRALIA
[b] Intelligent Polymer Research Institute, University of Wollongong, NSW 2522 AUSTRALIA

ABSTRACT

Conducting polymer actuators with favourable properties such as linearity, high power density and compliance are of increasing demand in micro applications. These materials generate forces over two times larger than produced by mammalian skeletal muscles. They operate to convert electro chemical energy to mechanical stress and strain. On the other hand, the application of conducting polymers is limited by the lack of a full description of the relation between four essential parameters: stress, strain, voltage and current. In this paper, polypyrrole helix tube micro actuator mechanical characteristics are investigated. The electrolyte is propylene carbonate and the dopant is TBA. PF_6. The experiments are both in isotonic and isometric conditions and the input parameters are both electrical and mechanical. A dual mode force and length control and potentiostat / galvanostat are utilized for this purpose. Ultimately, the viscoelastic behaviour of the actuator is presented in this paper by a standard stress relaxation test. The effect of electrical stimulus on mechanical parameters is also explored by cyclic voltametry at different scan rates to obtain the best understanding of the actuation mechanism. The results demonstrate that the linear viscoelastic model, which performed well on conducting polymer film actuators, has to be modified to explain the mechanical behaviour of PPy helix tube fibre micro actuators. Secondly, the changes in mechanical properties of PPy need to be considered when modelling electromechanical behaviour.

Keywords: conducting polymers, Polypyrrole, micro actuator, helix tube, fibre.

1. INTRODUCTION

The demand for micro scaled actuators is growing in micro robotics. In this application, conducting polymers (CPs) have useful characteristics compared to other materials: shape memory alloys, piezoelectric polymers, electro active gels [1, 2]. Previous research shows conducting polymers have competitive performance relative to other active materials with its muscle-like properties [3]. Polypyrrole (PPy) has outstanding actuation properties among conducting polymers, which makes it applicable in micro robotics and biomedical applications [4-6].

The investigation of actuation characteristics is significant for understanding how conducting polymers behave as micro actuators. The CP properties were divided into an actuation part and a viscoelastic part, which are then superimposed to model the behaviour of the actuator. The actuation strain was considered proportional to charge transferred and independent of mechanical strain. [7-9]. On the other hand, a viscoelastic lumped parameter method was developed to describe the mechanical behaviour of CP actuators [10, 11] and the model performance was verified both experimentally and using the complicated continuum mechanics method [11-13] based on Biot's poroelastic theory [14, 15].

Recently, it has been observed that there is interaction between the actuation strain and mechanical properties that are modified by electrical stimulus [16-20]. A better understanding of these interactions is needed to fully model the actuator performance.

In this paper, the viscoelastic linear model, which performed well on PPy film actuators, is generalised to describe the mechanical behaviour of PPy helix tube fibre actuators. The results demonstrate that the model has to be modified to be utilised as a consistent model and the electrical excitation and external mechanical load affect the model's linearity. For this purpose, the stress strain tests were arranged in different isometric strain steps to probe the effect of stretching on viscoelastic parameters. In the next step, investigation of the effect of electrical stimulus on the stiffness parameters has been carried out in isotonic condition and cyclic voltametric input at different scan rates. The results show that the

* chris_cook@uow.edu.au, phone: +61 2 4221 3062 and fax: +61 2 4221 3143

actuation effect, which is produced by diffusion of ions, is not negligible in predicting the behaviour of PPy helix tube micro fibre actuator.

2. MATERIALS AND METHODS

Propylene carbonate (PC) (Aldrich) and tetrabutylammonium hexafluorophosphate (TBA-PF_6, obtained from Sigma) both of AR grade were used. Pyrrole monomer from Merck was distilled and stored under −18 ◦C before use. Platinum wires in 250 and 50 µm diameter were from Goodfellow. The constant current required for polymerization was measured using an EG and G Princeton Applied Research Model 363 potentiostat / galvanostat.

PPy fibre was grown galvanostatically for 16 hours with a 0.15 [mA/cm^2] current density. Polymerization solution was PC containing 0.06M Pyrrole and 0.05M TBA-PF_6. The polymerization temperature was controlled around −25 to −28 °C. A two-electrode configuration was used; the working electrode was 250µm Pt wire tightly wound by 50µm Pt wire as helix; the auxiliary electrode was a stainless steel mesh. After growth, the 250µm Pt wire was pulled out leaving a hollow PPy fibre containing the thinner Pt wire embedded as a helix in the tube wall. Two pieces of 250µm Pt wire were inserted to each end of PPy helix tube to enable electrical connection and sealed by hot-melt polystyrene. PPy helix tubes were stored wet in PC containing 0.25M TBA-PF_6 before testing. Fig. 1 shows the actuator structure; further fabrication information is given in reference [21].

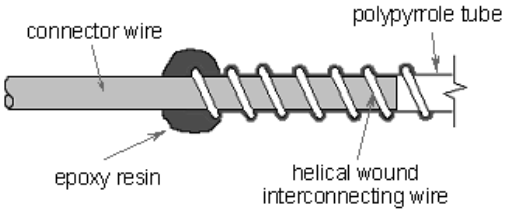

Fig. 1. Structure of PPy helix tube actuator.

Fig. 2 shows the arrangement of the test cell. The test cell consists of an actuator, which is connected as the working electrode, a counter electrode, an electrolytic solution, and a glass tube to contain everything. The tube is clamped in a position that is fixed relative to the lever-arm unit. One end of the actuator is fixed to the bottom end of the tube and the other end is connected to the lever arm and is free to move.

The reference electrode was Ag wire in 0.01M $AgNO_3$ and 0.1M TBA.PF_6 in acetonitrile (ACN) using 0.1M TBA.PF_6 in PC as a salt bridge. Fig. 3 displays their arrangement.

All the experimental data was processed and recorded by MacLab/4e AD instruments and computer. Isometric and isotonic conditions were applied using a force/length controller (Aurora Scientific, Dual Mode Model300B). This unit has four analogue input channels that were used to record the voltage and current generated by the potentiostat, and the force and position of the actuator, which was being measured by the lever-arm system. The input signals are then digitised and can be sampled at very high rates (up to 200 000Hz). The unit can also filter the signals if necessary, before passing them on to the computer. The resulting data is recorded on a personal computer using a software package known as Chart. Chart provides various options for processing and presenting the data; for example it allows the user to change the scaling or the sampling rate of the signal. There are two methods to simulate mechanical behaviour: Kelvin's and Maxwell's model [22]. The Kelvin model contains a spring and dashpot

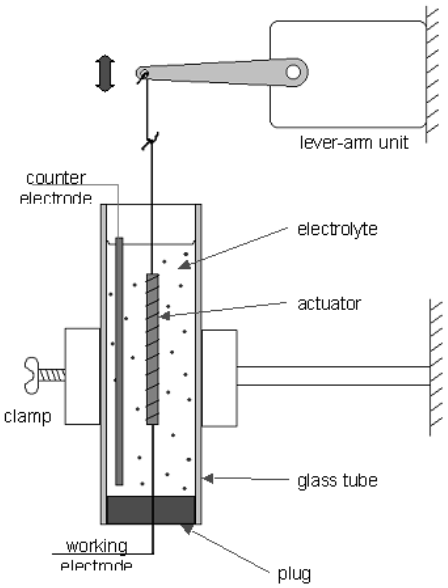

Fig. 2. Installation of actuator.

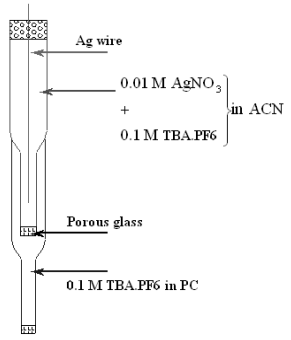

Fig. 3. Ag/Ag+ Reference electrode.

in parallel and Maxwell's model has these elements in series. Each approach has good performance in different tests. Maxwell's approach can model the stress-relaxation test and Kelvin's has good performance in estimating the creep test. It is possible to have a combination of both methods in one model, containing two springs and one dashpot, a spring in series with the dashpot and the other in parallel to both of them, which is known as the Standard Linear Solid model.

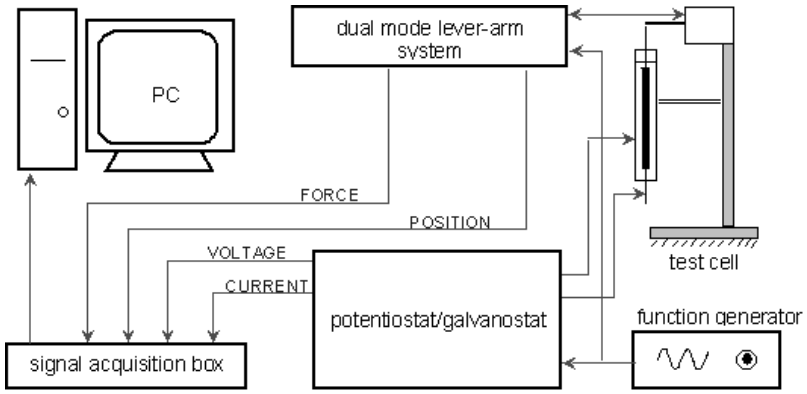

Fig. 4. Instruments configuration.

The polymer system can be considered as a configuration of many finite elements and each element can be modelled in Kelvin or Maxwell's mode. The result is simply many Kelvin's models in series or many Maxwell's in parallel. The Conducting Polymer actuator is assumed as a configuration of n Standard Linear Solid models, with the active strain generation term considered as a box in this circuit [10, 11]. This configuration and all the model parameters are shown in Fig. 5.

In this case, a step isometric strain is the system input and the stress response is defined as the output. The value of stress is computed for stress relaxation test in equation (1).

$$\sigma(t) = \varepsilon_{step}.\left(\left(\sum_{i=1}^{n} K_i.e^{-\frac{K_i}{\eta_i}.t}\right) + K_r\right) \qquad (1)$$

The initial and final value of the response stress are calculated by using the Final Value and Initial Value Theorem in (2)

$$\lim_{t\to\infty}(\sigma(t)) = \varepsilon_{step}.K_r$$

$$\lim_{t\to 0}(\sigma(t)) = \varepsilon_{step}.\left(\left(\sum_{i=1}^{n} K_i\right) + K_r\right) \qquad (2)$$

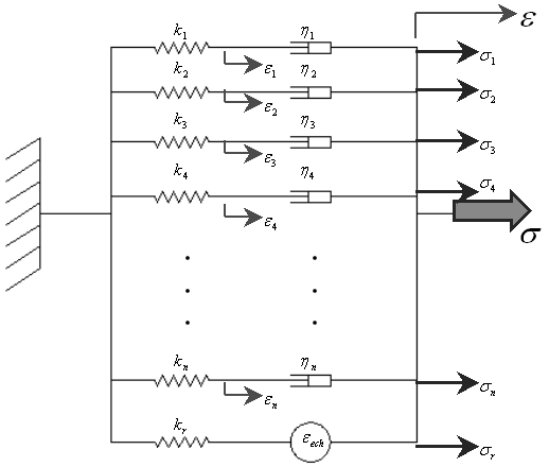

Fig. 5. Viscoelastic model of the actuator.

Seven stress-relaxation tests were performed with different isometric strain inputs. The model, which was described in (1) and Fig. 5, was utilized to explain the viscoelastic behaviour of a PPy helix tube actuator. The curve fitting technique applied to calculate the parameters used Trust-Region methods for Nonlinear Minimizing in the MATLAB® curve fitting toolbox; further information is referred to in references [23, 24].

3. RESULTS

The viscoelastic parameters of stiffness and damping coefficient were determined from stress relaxation tests at different input strain levels. For linear viscoelastic materials, these parameters are independent of the applied strain in stress relaxation tests. However, as shown in Fig. 6, total stiffness coefficient increases with increasing strain. This increase appeared linear with high regression factor (0.9782) in the strain range used in actuator tests (<1% initial strain). The residual stiffness (Kr) shows a similar trend with increasing input strain. The stiffness coefficients of the individual Maxwell elements are not strongly affected by the strain applied.

The fitted parameters show that the PPy helix tube actuators become stiffer at higher input strains. The reason for this seemingly anomalous behaviour can be determined from the non-linear stress/strain curve for these materials (Fig. 7). These curves are parabolic to strains of 1-2% due to the fact that these high aspect ratio fibres are not perfectly straight at zero strain. Thus, relatively large strains occur at small stresses due to the bending and straightening of the helix tube fibres. This non-linear stress-strain region extended to higher strains when longer fibres were used. As stated above, these actuators are used at initial strains of <1%. Thus, the modelling of the actuators must take into account their changing stiffness coefficients in this strain range. Fortunately, the change in stiffness is approximately linear, so the stiffness at any strain can be determined readily from the data given in Fig. 6.

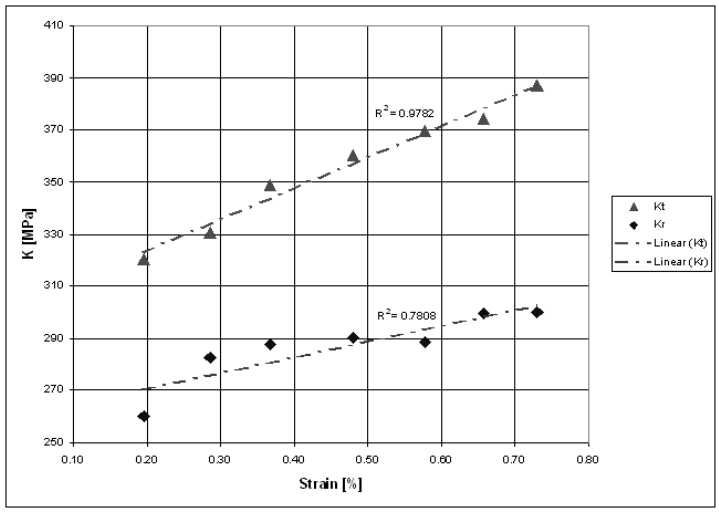

Fig. 6. Variation of stiffness coefficients vs. input isometric strain.

The damping coefficients are similarly affected by the magnitude of the input strain, as shown in Fig. 8. Up to a strain of ~0.6% the damping coefficient increases and then remains approximately constant. The first Maxwell branch dominates the total damping, with smaller contributions from the third and second branches. The straightening of the helix tube fibre at small strains is likely to be the cause of the increasing damping coefficient. In linear viscoelastic materials these coefficients are independent of strain. Fortunately in the present case, the damping coefficients change in an approximately linear fashion with strain. The linear relationship means that the coefficients can be readily calculated from the data given in Fig. 6.

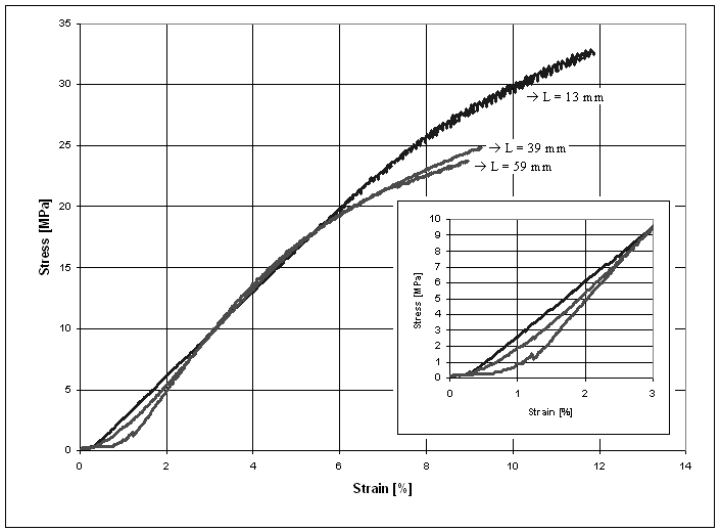

Fig. 7. Stress-strain curves for different length of actuator.

Additionally, it would be useful to investigate the variation of the time constant parameters, which were computed using the equation (3). Fig. 9 contains these values.

$$\tau_i = \frac{\eta_i}{K_i} \tag{3}$$

The time constants depend on the applied strain since both the K and η terms are strain dependent. The relaxation times are rather long indicating that creep should not affect the helix tube actuators at fast switching speeds (e.g. >1 Hz) but will be important for slower processes, including DC control.

To investigate the effect of electrical stimulus on the polymer stiffness, a high frequency isotonic stress was applied to the material and the initial strain response measured. The pulse-applied stress eliminates the effect of actuation strain and the equipment applies a step input within a period of time close to their sampling time so the effect of actuation strain approaches zero. Undoubtedly, the other parameters can also be calculated by curve fitting to the response plot, which is complicated and not required in this work.

The results illustrate the large effect of actuation voltage on the total stiffness. The change in stiffness was more than 20 percent. Fig. 10 shows the modulus variation with strain and voltage. The plot of strain also shows the value of passive strain relative to active strain. The modulus plot was smoothed by moving average method [23].

Fig. 11 shows this stiffness variation along with the cyclic voltametric diagram, showing the diffusion effect on passive mechanical properties. The scan rate in these tests was 1 mV/s, which is one of the several results obtained with different scan rates. Fig. 12 shows the variation of stiffness coefficient at different scan rates. There is a direct relationship between the doping level variation, which causes the active strain to be generated, and total stiffness of the actuator. These results illustrate that the mechanical parameter follows the variations of the active strain over the CV diagram.

Fig. 12 shows that increasing the frequency of applied voltage decreases the effect on stiffness modulus variation. The frequency effect is because of the decreasing active strain value with increasing applied frequency. The similarity in behaviour suggests a similar basic mechanism that affects both the active strain and the material stiffness. Diffusion of ionic species (and solvent) into the polymer can describe both effects as well as the frequency dependence.

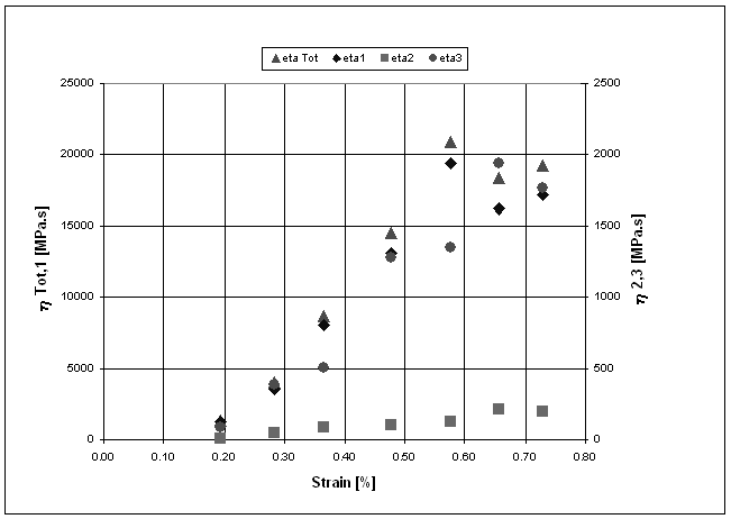

Fig. 8. Damping ratios variation.

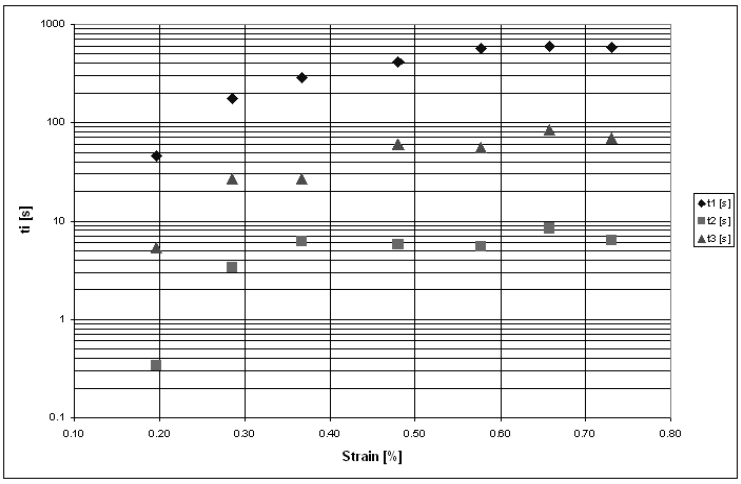

Fig. 9. Time constants vs. strain.

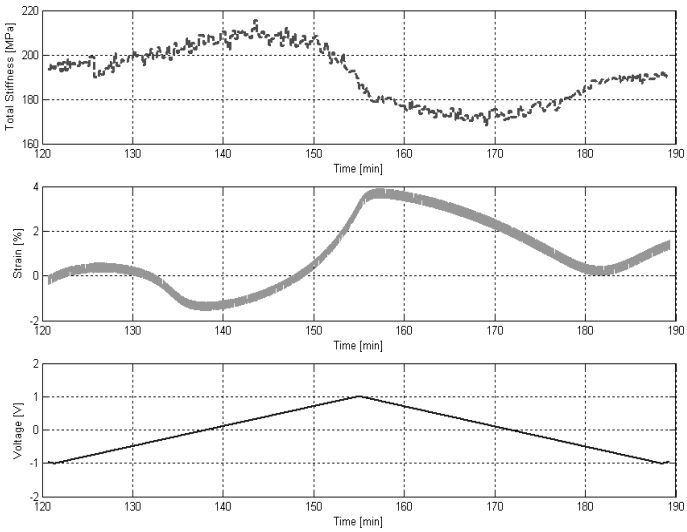

Fig. 10. Effect of actuation on total stiffness coefficient.

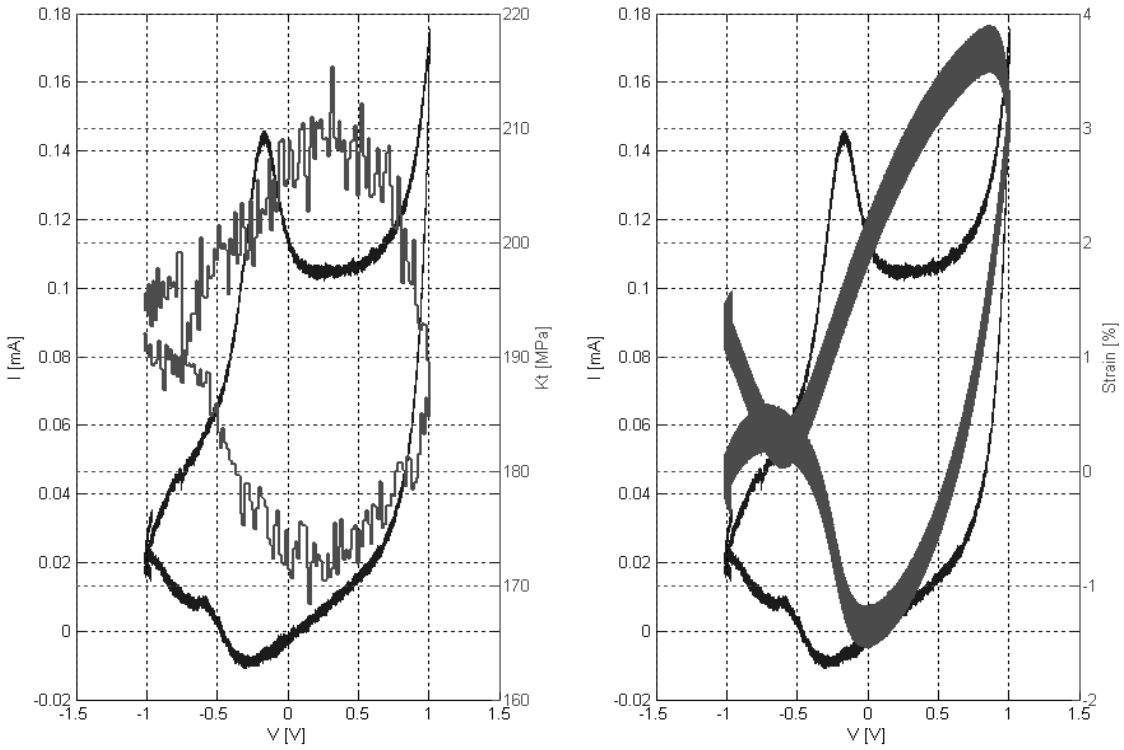

Fig. 11. CV diagram and stiffness changing over actuation.

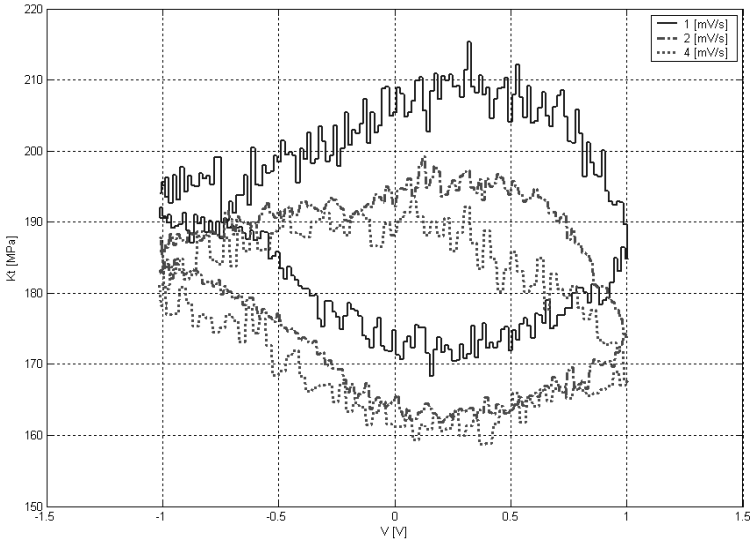

Fig. 12. Stiffness variation during actuation in different scan rates.

4. CONCLUSION

The Lumped Parameters technique [10, 11, 19] was applied to a PPy helix tube actuator and utilized to describe the viscoelastic behaviour. The results demonstrate that the linear models cannot estimate the mechanical behaviour of PPy fibre, although they are successful on conducting polymer films [10-13, 19]. Subsequently, the wet stress relaxation test at zero volts (relative to reference electrode) was carried out and the mathematical model fitted to the data to give values of stiffness and damping coefficients calculated under different test conditions. It was shown that both stiffness and damping coefficients varied for different applied isometric strains, but the graphs illustrate that the variations are almost linear. This means that the stress-strain diagram is parabolic in the actuation strain area, giving an S-shaped curve over the entire strain range. This behaviour makes the dynamic explanation of the fibre actuators very complicated, because the phenomenon of active strain generation of conducting polymer fibres is modelled as a configuration of many springs and dashpots which do not behave like linear elements. Hence, all elements of the system would be altered during displacement under the effect of electrical stimulation. Thus the system proposed here moves through different isometric strain conditions during the process of actuation and consequently the characteristics of system elements vary during the stimulation. However, this variation is predictable linearly and these linear methods can be generalized for PPy fibre actuators.

In another study, a PPy fibre actuator was stimulated with a triangular voltage at different frequencies while total stiffness was measured. In the research presented here a high frequency square wave isotonic stress is employed to compute the total stiffness value. The results reveal that the effect of the activation process for EAP actuators on mechanical properties cannot be neglected. Results demonstrate that there is a direct relationship between doping level variation and total stiffness of the actuator. The graph, which presents cyclic voltametric results against the variation of total stiffness, illustrates that the mechanical parameters follows the variations of the CV diagram. For example, when there is a peak of oxidation there will be a peak of stiffness. These results show that the parameters of the system change while the process of strain generation starts. This effect reduces at higher frequencies of stimulation.

REFERENCES

1. Baughman, R.H., Conducting polymer artificial muscles. Synthetic Metals, 1996. 78(3): p. 339-353.
2. Smela, E., O. Inganas, and I. Lundstrom, Conducting polymers as artificial muscles: challenges and possibilities. Journal of Micromechanics & Microengineering, 1993. 3(4 Dec): p. 203-205.
3. Hunter, I.W. and S. Lafontaine. A comparison of muscle with artificial actuators. in Solid-State Sensor and Actuator Workshop, 1992. 5th Technical Digest., IEEE. 1992.
4. Jager, E.W.H., et al., Applications of polypyrrole microactuators. Proceedings of Spie - the International Society for Optical Engineering, 1999. 3669: p. 377-384.
5. Jager, E.W.H., et al., Polypyrrole microactuators. Synthetic Metals, 1999. 102(1-3 pt 2 Jun): p. 1309-1310.
6. Smela, E., Conjugated polymer actuators for biomedical applications. Advanced Materials, 2003. 15(6 Mar 17): p. 481-494.
7. Penner, R.M., L.S.V. Dyke, and C.R. Martin, Electrochemical Evaluation of Charge-Transport Rates in Polypyrrole. journal of Physical Chemistry, 1988. 92: p. 5274-5282.
8. Penner, R.M. and C.R. Martin, Electrochemical Investigations of Electronically Conductive Polymers. 2. Evaluation of Charge-Transport Rates in Polypyrrole Using an Alternating Current Impedance Method. journal of Physical Chemistry, 1988. 93(2): p. 984-989.
9. Penner, R.M., L.S. Van Dyke, and C.R. Martin, Electrochemical evaluation of charge-transport rates in electronically conductive polymers. Solid State Ionics, 1989. 32-33(pt 1 Feb-Mar): p. 553-566.
10. Della Santa, A., D. De Rossi, and A. Mazzoldi, Characterization and modelling of a conducting polymer muscle-like linear actuator. Smart Materials & Structures, 1997. 6(1 Feb): p. 23-34.
11. Mazzoldi, A., A. Della Santa, and D. De Rossi, Chapter 7: Conducting Polymer Actuators: Properties and Modeling, in Polymer Sensors and Actuators, Y. Osada and D.D. Rossi, Editors. 2000, Springer Verlag. p. 207-244.
12. Della Santa, A., et al., Conducting polymer electromechanics: a continuum model of passive mechanical properties. Proceedings of SPIE - The International Society for Optical Engineering, Bellingham, WA, 1996. 2779: p. 371-376.

13. Della Santa, A., et al., Passive mechanical properties of polypyrrole films: A continuum, poroelastic model. Materials Science and Engineering: C, 1997. 5(2): p. 101-109.
14. Biot, M.A., General Theory of Three-Dimensional Consolidation. Journal of Applied Physics, 1941. 12(2): p. 155-164.
15. Biot, M.A., Theory of Elasticity and Consolidation for a porous Anisotropic Solid. Journal of Applied Physics, 1955. 26(2): p. 182-185.
16. Spinks, G.M., et al., Strain Response from Polypyrrole Actuators under Load. Advanced Functional Materials, 2002. 12(6-7): p. 437-440.
17. Spinks, G.M., et al., Enhanced control and stability of polypyrrole electromechanical actuators. Synthetic Metals, 2004. 140: p. 273-280.
18. Spinks, G.M., et al., The amounts per cycle of polypyrrole electromechanical actuators. Smart Materials & Structures, 2003. 12(3 June): p. 468-472.
19. Della Santa, A., D. De Rossi, and A. Mazzoldi, Performance and work capacity of a polypyrrole conducting polymer linear actuator. Synthetic Metals, 1997. 90(2): p. 93-100.
20. Chiarelli, P., et al., Actuation properties of electrochemically driven polypyrrole free-standing films. Journal of Intelligent Material Systems & Structures, 1995. 6(1 Jan): p. 32-37.
21. Ding, J., et al., High performance conducting polymer actuators utilising a tubular geometry and helical wire interconnects. Synthetic Metals, 2003. 138(3): p. 391-398.
22. Ebewele, R.O., Polymer science and technology. Vol. 1. c2000, London: Boca Raton. 483.
23. Moré, J.J. and D.C. Sorensen, Computing a Trust Region Step. SIAM Journal on Scientific and Statistical Computing, 1983. 3: p. 553-572.
24. Draper, N.R. and H. Smith, Applied Regression Analysis. 3rd ed. 1998, New York: John Wiley & Sons.